Optimization of a Deep-Space Ka-Band Link Using Atmospheric-Noise-Temperature Statistics

S. Shambayati[1]

Statistics for atmospheric-noise-temperature data at a 31.4-GHz frequency were calculated for the Madrid and Goldstone Deep Space Communications Complexes from the data collected by the water vapor radiometer. These data consist of 74 months of measurements at Madrid and 46 months of measurements at Goldstone. The statistics then were used to optimize a deep-space 32-GHz (Ka-band) link at each site in terms of return data volume at a 30-deg elevation. The atmospheric-noise value obtained through this optimization then was used to calculate the Ka-band return-data volume advantage over 8.4 GHz (X-band) as a function of elevation for a 34-m beam-waveguide antenna at each site. It was observed that, for both sites, the Ka-band advantage is maximized at a 60-deg elevation, providing from 7 to 8.4 dB more data than that provided by a 90 percent weather X-band link, depending on the antenna configuration. At lower elevations, this advantage is reduced to 4 to 5 dB. Finally, the average return-data volume advantage for Ka-band was calculated over two actual elevation trajectories. For the high-elevation trajectory, Ka-band offers an advantage of 6.5 to 7.8 dB more data volume at Madrid and 6.6 to 7.9 dB more at Goldstone, depending on the antenna configuration. For the low-elevation trajectory, Ka-band offers an advantage between 5.7 and 6.8 dB in Madrid and between 5.7 and 6.9 dB at Goldstone.

I. Introduction

In order to evaluate the performance of a data link, the total data-return volume of the link must be analyzed. For a fixed bit-signal-to-noise ratio, E_b/N_0, requirement for the link, the data rate and, hence, the total data volume, are inversely proportional to the system-noise temperature, T_{op} [1,2]. Several factors contribute to T_{op}. At 32 GHz (Ka-band), the most important of these factors is the atmospheric-noise temperature, T_{atm}. At Ka-band, T_{atm} is severely affected by the variations in the atmosphere's water content. Therefore, bad weather or high humidity could severely degrade the performance of the link at Ka-band.

Atmospheric-noise temperature, T_{atm}, is measured at Deep Space Communications Complex (DSCC) 10 (Goldstone) and DSCC 60 (Madrid) using a water vapor radiometer (WVR). The WVR data are very accurate (± 0.5 K for clear conditions and ± 1 K for cloudy conditions)[2] and can be used

[1] Communications Systems and Research Section.

[2] S. Keihm, personal communication, Microwave and Lidar Technology Section, Jet Propulsion Laboratory, Pasadena, California, 1997.

to calculate the effects of T_{atm} on T_{op} and, therefore, on the data volume. The data used to obtain the results in this article were gathered at DSCC 60 over 74 months (September 1990 through December 1996, excluding February 1991 and May 1992) and at DSCC 10 over 46 months (October 1993 through September 1997, excluding December 1995 and February 1996). Probability distributions for these measurements were obtained for each month at each site. Based on these distributions, the maximum data-return volume for each month at each site was calculated, and the Ka-band link advantage over 8.4 GHz (X-band) was estimated.

In the following sections, the details of this analysis are presented. In Section II, the nature of the data is discussed and the process of generating the statistics for the data is presented. In Section III, calculations for the data-return volume from the WVR measurements are explained, and, in Section IV, the statistical results are discussed. In Section V, results for the Ka-band link advantage over X-band are presented. Section VI presents the conclusions.

II. The WVR Data

The WVR data used for this analysis were gathered from September 1990 through December 1996, excluding February 1991 and May 1992, at DSCC 60 and from October 1993 through September 1997, excluding December 1995 and February 1996, at DSCC 10. These data sets contain measurements of the atmospheric-noise temperature at a 30-deg elevation with cosmic-background noise. The elevation of 30 deg was selected in order to evaluate the link at typical tracking elevation angles. For the analysis in this article, the cosmic-background noise was removed from the data. The data at DSCC 60 were gathered at the nominal rate of one measurement every 30 min and more frequently when the WVR was in continuous tip-curve mode. The data at DSCC 10 were gathered at the rate of approximately one measurement every 3.6 min. However, due to interference from other non-weather-related sources, sometimes the data points were tagged as bad and were not used in the statistics.

For data collected at DSCC 60, each data point represents T_{atm} measurements integrated over a 10-min period except for when the WVR was operating in the continuous tip-curve mode. For analysis purposes, each data point is representative of 10 min of time except for when the time tag for a data point is less than 10 min greater than the time tag for the previous data point. In this case, it is assumed that the data point represents the T_{atm} measurements integrated over the period between the two time tags. For the data at DSCC 10, each data point represents 3.6 min of time unless the difference between the time tags is less than 3.6 min. In that case, it is assumed that the data point represents the time between its time tag and the time tag of the previous data point. Using these assumptions, time-weighted statistics of the data for each month, of the complete data set, and of the data for each month aggregated over the years were obtained.

III. Data Analysis

The first step in analyzing the data is to create a histogram (hence, a probability distribution) for each of the months. The histogram is created in a time-weighted fashion—that is, the period of time for which a temperature measurement is valid is added to the value of the bin into which that measurement falls. From the histogram, a cumulative probability distribution for each month is calculated. In addition, aggregate histograms and distributions for each month and for the complete data set were generated.

After the histogram is obtained for each time period, the maximum data-volume return is calculated. It is assumed that the system-noise temperature is T_{atm} plus equipment (amplifier-plus-antenna)-noise temperature and the cosmic-background noise. For this analysis, the equipment-noise temperature plus the cosmic-background noise was assumed to be 25 K. Also, for normalization purposes, it was assumed that the total data volume per unit time at $T_{op} = 1$ K and zero atmospheric loss is 100. Therefore, for any atmospheric noise temperature, T_{atm}, the maximum data volume possible is given by

$$V_d(T_{atm}) = \frac{100 \times L(T_{atm})}{25 + T_{atm}} \tag{1}$$

where $L(T_{atm})$ is the atmospheric loss factor at T_{atm} and is approximated by [3]

$$L(T_{atm}) \approx \frac{275 - T_{atm}}{275} \tag{2}$$

Given these assumptions, there are several measures that are useful for evaluating the data-volume return for each month. The first of these is the "genie" data volume. The genie data volume assumes that perfect prediction of the atmospheric-noise temperature is possible and that the data rate on the spacecraft can be instantaneously adjusted so that the received signal-to-noise ratio (SNR) on the ground allows for an acceptable bit-error rate (BER) while maintaining maximum data throughput.

To calculate the genie data volume for each time period, let T_n be the nth T_{atm} temperature measurement for that time period and let t_n be the time duration for which this measurement is applicable. Then, the genie data volume is calculated according to the following:

$$V_g = \frac{\sum\limits_n \frac{100 \times L(T_n) \times t_n}{25 + T_n}}{\sum\limits_n t_n} \tag{3}$$

The genie data volume is the upper bound on the data volume that could be obtained for any given time period. However, since perfect weather prediction is not possible, the link is designed by selecting a single atmospheric-noise temperature value. Let $F_{atm}(T) = \Pr\{T_{atm} \leq T\}$ be the cumulative distribution function of the T_{atm} for a given period. Then, for a design atmospheric-noise temperature, T_d, the total data-volume return is given by

$$V_{tot}(T_d) = \frac{100 \times L(T_d) \times F_{atm}(T_d)}{25 + T_d} \tag{4}$$

The optimum design temperature, T_{opt}, is that temperature which maximizes $V_{tot}(T_d)$; in other words,

$$T_{opt} \ni T_{tot}(T_{opt}) \geq V_{tot}(T_d) \,\forall\, T_d \tag{5}$$

The maximum data-return volume is, therefore,

$$V_{max} = V_{tot}(T_{opt}) \tag{6}$$

For the analysis in this article, the following quantities are evaluated for each month: T_{opt}, V_{max}, $F_{atm}(T_{opt})$, V_g, $V_d(T_{opt})$, $V_d(\overline{T}_{opt})$, $V_d(T_{opt}^{(tot)})$, and $V_d\left(T_{opt}^{(x)}\right)$. The $\overline{T}_{opt}$ is the average of T_{opt} for each site; $T_{opt}^{(tot)}$ is the optimal temperature evaluated over all months for each site; and $T_{opt}^{(x)}$ is the aggregate optimum temperature for month x (e.g., $T_{opt}^{(\mathrm{May})}$ is the optimum temperature evaluated over all the data for the months of May).

IV. Statistical Results

The results of the statistical analysis of the data are presented in Figs. 1 through 7. Figures 1(a) and 1(b) represent the 80 and 99 percent temperatures for each month for Madrid and Goldstone, respectively. As we can see from these figures, while the 99 percent temperature varies widely, the 80 percent temperature remains relatively constant over the months, with the Madrid 80 percent temperature generally staying below 40 K and the Goldstone 80 percent temperature generally staying below 30 K. This indicates two things: first, that the weather affects Ka-band less than 20 percent of the time and, second, that Madrid is, in general, more humid than Goldstone.

Figures 2(a) and 2(b) represent T_{opt} and $F_{atm}(T_{opt})$ for each month for Madrid and Goldstone, respectively. Figure 2(a) indicates that the T_{opt} values for Madrid are mostly between 30 and 40 K and those of $F_{atm}(T_{opt})$ are mostly between 80 and 90 percent. Figure 2(b) indicates that the T_{opt} values for Goldstone are mostly around 30 K and that $F_{atm}(T_{opt})$ is mostly around 90 percent. A quantitative presentation of this observation is given in Table 1.

As we can see from Table 1, $\overline{T}_{opt}$ and $T_{opt}^{(tot)}$ values are close to each other for both sites. Similarly, $\overline{F_{atm}(T_{opt})}$ and $F_{atm}\left(T_{opt}^{(tot)}\right)$ are also close. Any difference between the values is attributed to the fact that the number of data points varies from month to month.

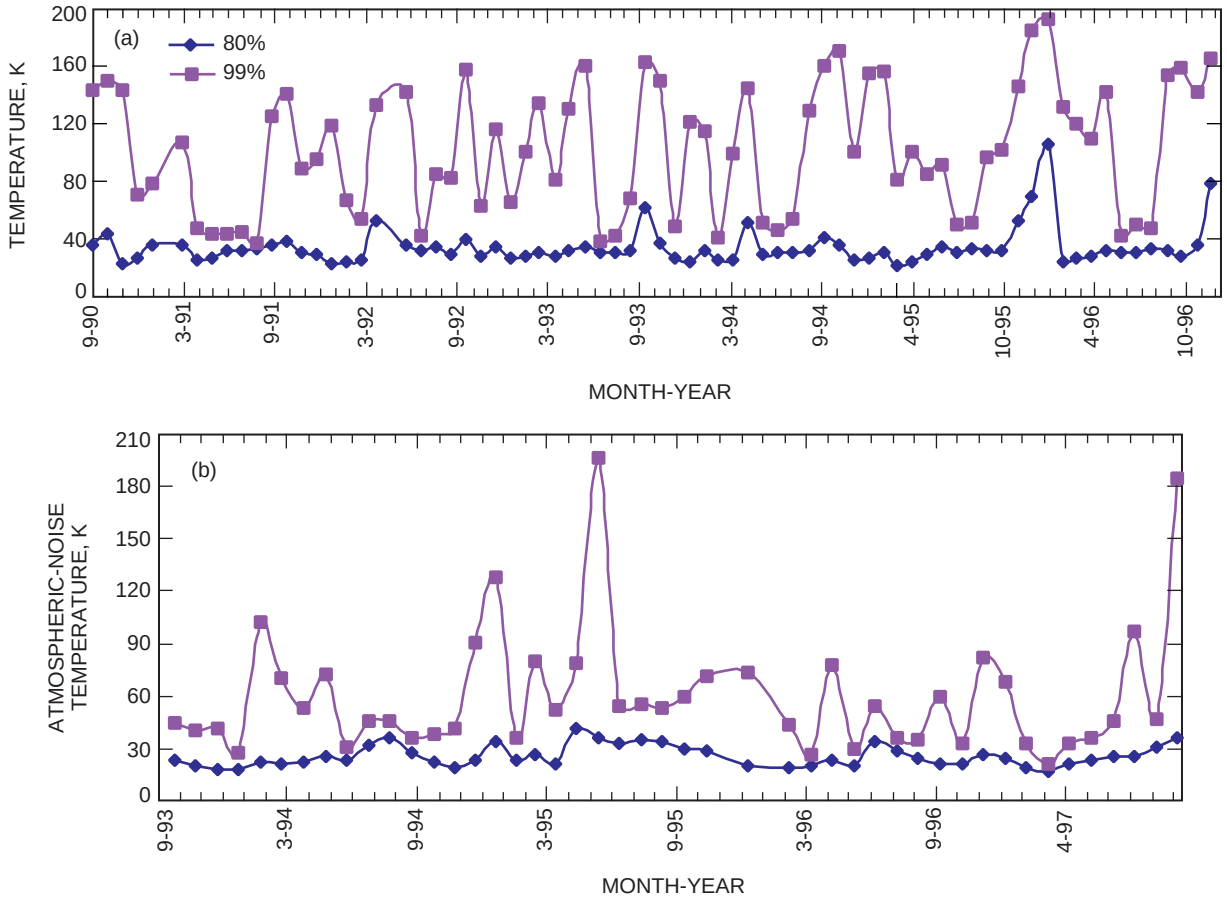

Fig. 1. Monthly 80 and 99 percent atmospheric-noise-temperature measurements: (a) Madrid from September 1990 through December 1996 and (b) Goldstone from October 1993 through September 1997.

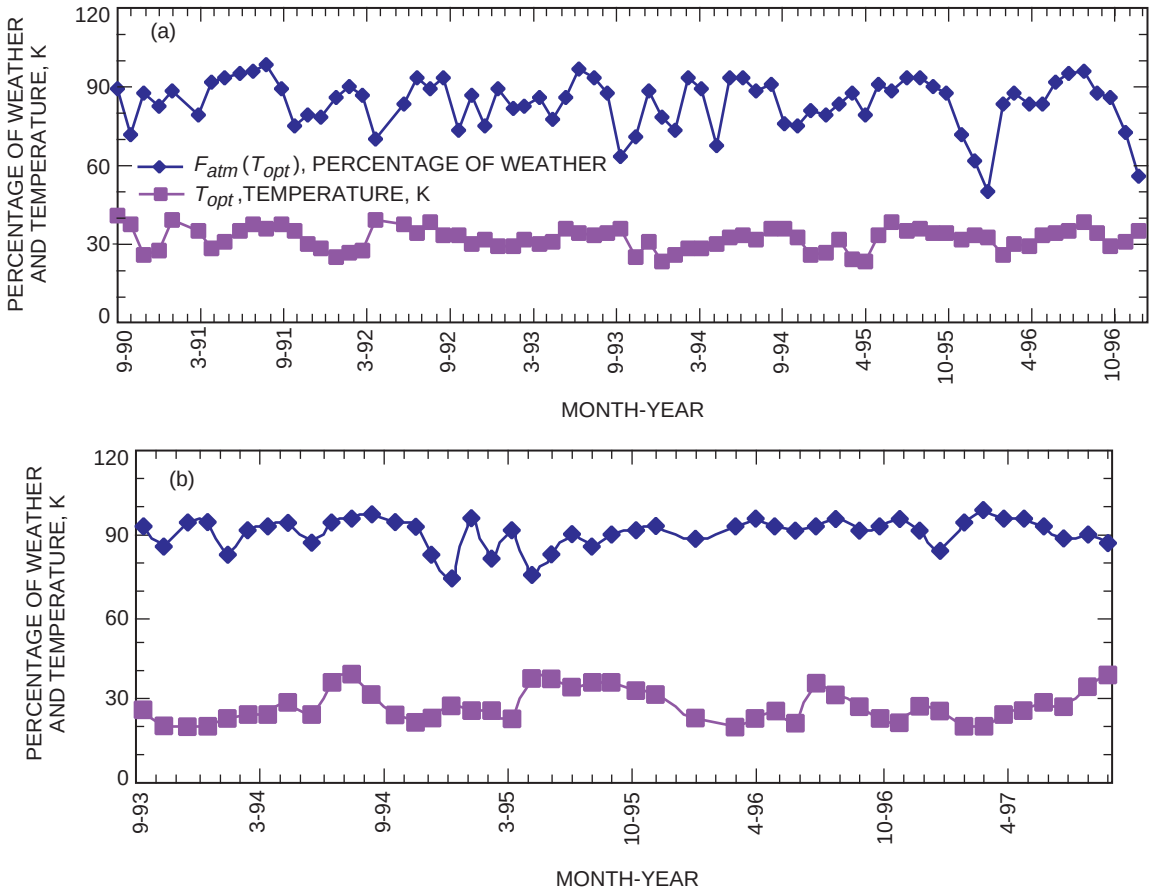

Fig. 2. Optimum percentage of weather and atmospheric-noise temperature: (a) Madrid from September 1990 through December 1996 and (b) Goldstone from October 1993 through September 1997.

Table 1. Average and aggregate optimum temperatures.

Site	$\overline{T}_{opt}$, K	$\overline{F_{atm}(T_{opt})}$, percent	$T_{opt}^{(tot)}$, K	$F_{atm}\left(T_{opt}^{(tot)}\right)$, percent
Madrid	32.05	83.82	34.00	84.07
Goldstone	27.67	90.30	31.63	88.78

Figures 3 through 5 provide us with an understanding of monthly variations at each site. Figures 3(a) and 3(b) show $T_{opt}^{(x)}$ and $F_{atm}\left(T_{opt}^{(x)}\right)$ over the year for each site, respectively. Figure 3(a) indicates that $T_{opt}^{(x)}$ for Madrid varies between 25.75 K (January) and 36.25 K (August and September) and that $F_{atm}\left(T_{opt}^{(x)}\right)$ varies between 73.5 percent (January) and 94.5 percent (July). Figure 3(b) indicates that $T_{opt}^{(x)}$ for Goldstone varies between 23.88 K (March) and 37.13 K (August) and that $F_{atm}\left(T_{opt}^{(x)}\right)$ varies between 83.1 percent (January) and 93.98 percent (April). This indicates that, in the design of the Ka-band link, it is *beneficial to take into account the monthly variations.* Figures 4(a) and 4(b) present the ordering of the months according to the amount of data returned when $T_{opt}^{(x)}$ is used as the design T_{atm}

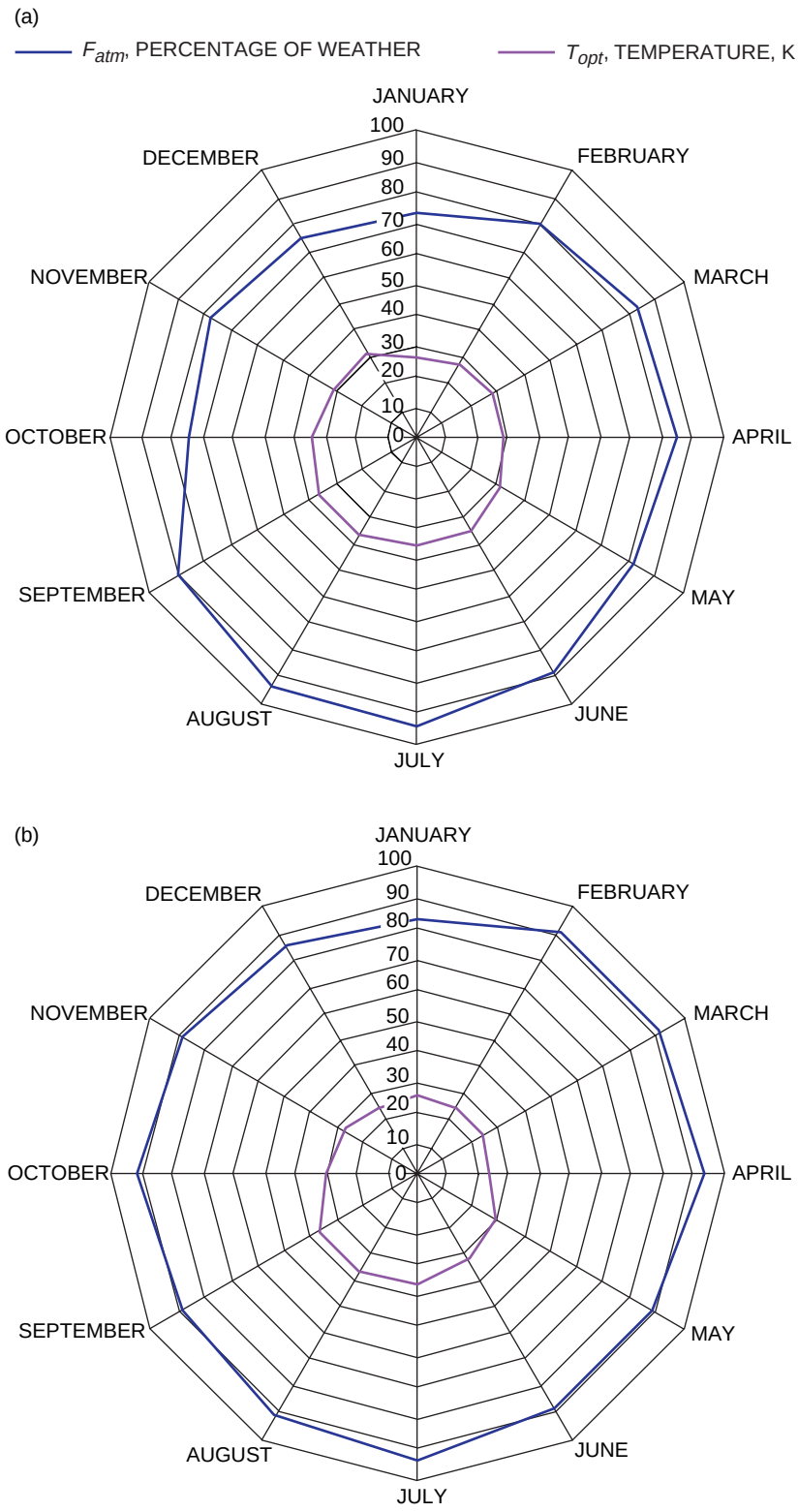

Fig. 3. Aggregate monthly optimum percentage of weather and atmospheric temperature: (a) Madrid from September 1990 through December 1996 and (b) Goldstone from October 1993 through September 1997.

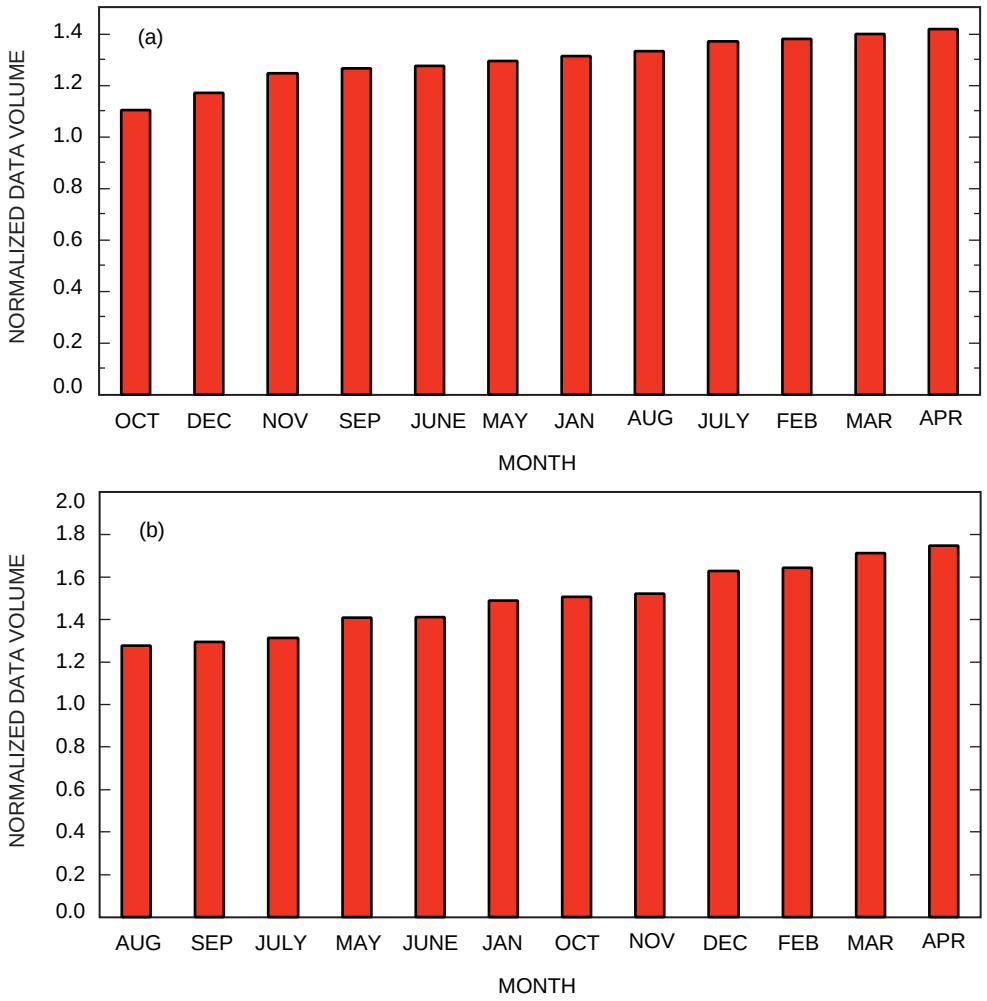

Fig. 4. Ordering of the months according to data-volume return: (a) Madrid from September 1990 through December 1996 and (b) Goldstone from October 1993 through September 1997.

for Madrid and Goldstone, respectively. As we can see from these figures, the best months for receiving Ka-band at Madrid are in late winter and early spring (February, March, and April), and the worst months are in late summer and autumn (September through December), with the worst month being October. For Goldstone, the best months are again in late winter and early spring (February, March, and April), while the worst months are in the summer (July, August, and September). Figures 5(a) and 5(b) represent variations in $F_{atm}(T_{opt})$ and T_{opt}, respectively, on a month-to-month basis for Madrid. As expected, these figures show a direct correlation between variation of T_{opt} and $F_{atm}(T_{opt})$. The month with the least amount of variation is July, while January shows the most variation. This means that the link is most predictable in July and least predictable in January. Furthermore, Fig. 5(b) shows a slight seasonal variation in T_{opt}. As we can see from this figure, from May to October, T_{opt} is above 30 K while, from November to April, it is below 30 K. Furthermore, we note that from May through August the standard deviation of T_{opt} is small. This indicates that the weather during these months is not affected by severe weather systems. The increase in the standard deviation of T_{opt} from September through January indicates that the probability of having severe weather systems in these months increases accordingly. There is also a rise in the standard deviation of T_{opt} in March and April. This corresponds to the likely early spring showers. Figures 5(c) and 5(d) show the variations in $F_{atm}(T_{opt})$ and T_{opt}, respectively, on a month-to-month basis for Goldstone. These figures show less of a month-to-month variation than that

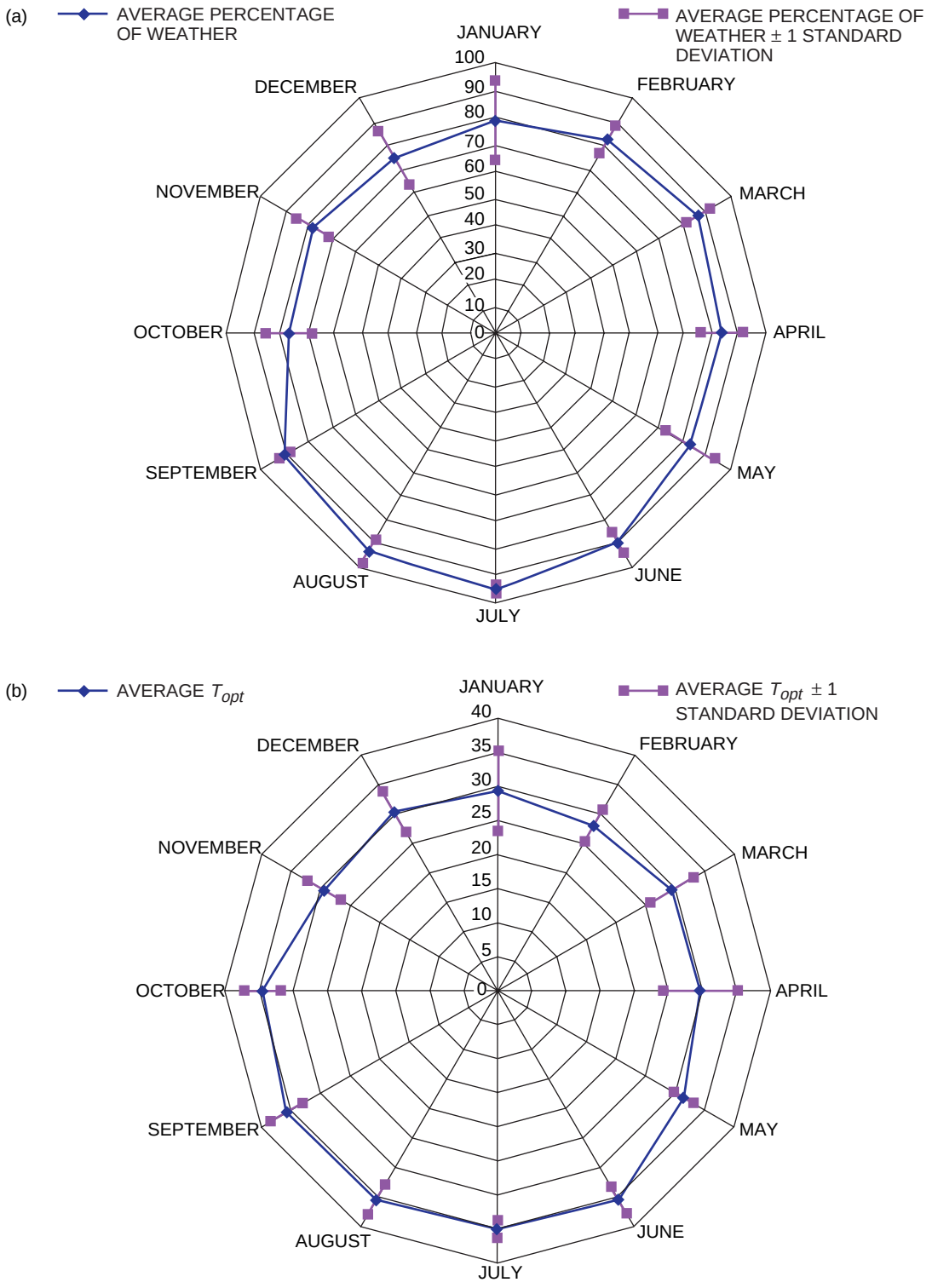

Fig. 5. Month-to-month variations in F_{atm} (T_{opt}) and T_{opt}: (a) Madrid mean monthly optimum percentage of weather and mean percentage of weather ± 1 standard deviation, (b) Madrid mean monthly T_{opt} and mean T_{opt} ± 1 standard deviation, (c) Goldstone mean monthly optimum percentage of weather and mean percentage of weather ± 1 standard deviation, and (d) Goldstone mean monthly T_{opt} and mean T_{opt} ± 1 standard deviation.

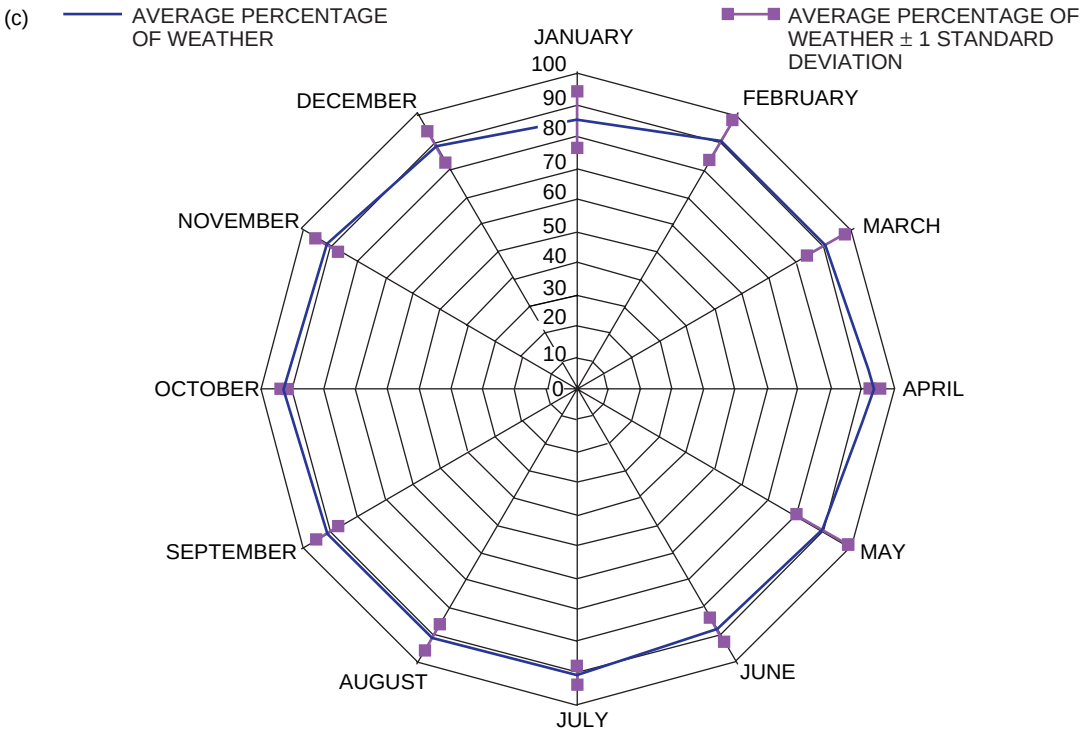
(c)
AVERAGE PERCENTAGE OF WEATHER
AVERAGE PERCENTAGE OF WEATHER ± 1 STANDARD DEVIATION
JANUARY
FEBRUARY
MARCH
APRIL
MAY
JUNE
JULY
AUGUST
SEPTEMBER
OCTOBER
NOVEMBER
DECEMBER
100
90
80
70
60
50
40
30
20
10
0

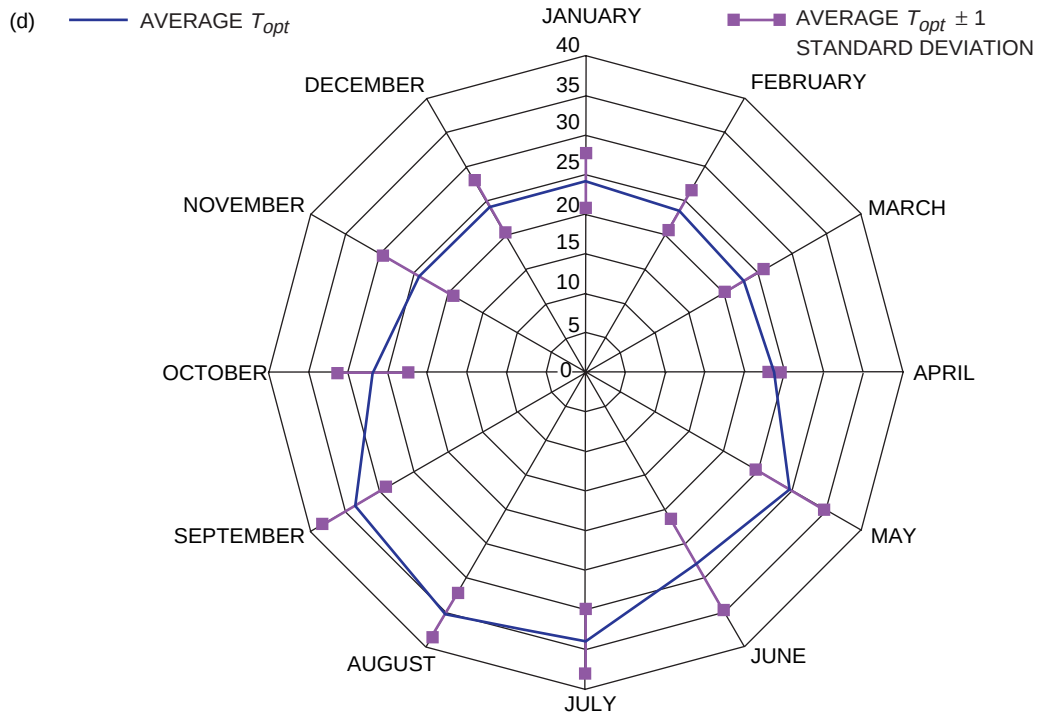
(d)
AVERAGE T_{opt}
AVERAGE T_{opt} ± 1 STANDARD DEVIATION
JANUARY
FEBRUARY
MARCH
APRIL
MAY
JUNE
JULY
AUGUST
SEPTEMBER
OCTOBER
NOVEMBER
DECEMBER
40
35
30
25
20
15
10
5
0

Fig. 5 (contd).

shown in Figs. 5(a) and 5(b). However, they show a larger seasonal trend in the value of T_{opt}. This is attributed to the fact that Goldstone has basically two seasons: dry and cool with some variations due to storms in the winter and spring, and hot and humid during summer and autumn. Furthermore, this indicates that it is more beneficial to use seasonal numbers for the design of Ka-band links at Goldstone.

Figure 6 shows the cumulative atmospheric-noise temperature distribution for the complete data set at each site. As we can see from this figure, Goldstone is drier overall than Madrid. The 90 percentile aggregate atmospheric-noise temperature, $T_d^{(90\%)}$, for Madrid is 40.16 K, while the same for Goldstone is 32.32 K.

Figures 7(a) and 7(b) show the data-return volume when the optimum atmospheric-noise temperature, T_{opt}; the aggregate monthly optimum temperature, $T_{opt}^{(x)}$; the aggregate optimum temperature, $T_{opt}^{(tot)}$; the average of the optimum atmospheric-noise temperatures, $\overline{T}_{opt}$; and the 90 percentile aggregate atmospheric-noise temperature, $T_d^{(90\%)}$, are used for the link design atmospheric-noise temperature, T_d, as well as the genie data volume. The results shown in these figures are summarized in Table 2.

As we can see from Table 2, the more time specific the optimization of T_d, the more data are returned. Note that, at Goldstone, $\overline{V_{tot}(\overline{T}_{opt})}$ is less than $\overline{V_{tot}\left(T_d^{(90\%)}\right)}$. This is due to the fact that $T_d^{(90\%)}$ is much closer to $T_{opt}^{(tot)}$ than is $\overline{T}_{opt}$. Furthermore, note that, under the best possible scenario, when T_{opt} is used for T_d, the average data-volume return is only 74 percent of the average genie data volume for Madrid and 80 percent of the average genie data volume for Goldstone. This indicates that, if a weather-prediction system is employed, the return-data volume could be further increased. In addition, note that the difference between $\overline{V_{tot}\left(T_{opt}^{(x)}\right)}$ and $\overline{V_{tot}\left(T_{opt}^{(tot)}\right)}$ is greater for Goldstone than for Madrid (0.26 dB for Goldstone versus 0.1 dB for Madrid). This is due to the fact that Goldstone experiences relatively larger seasonal variations, as indicated by Figs. 3(b), 5(c), and 5(d). Finally, note that more data are returned at Goldstone than at Madrid, due to Goldstone's drier weather.

V. Ka-Band Data-Volume Advantage over X-Band for the 34-m Beam-Waveguide (BWG) Antennas at Madrid and Goldstone

In the previous section, we used the data obtained to maximize the average return-data volume on a Ka-band link at a 30-deg elevation for the Madrid and Goldstone sites. In this section, we will focus on the return data-volume advantage of a 34-m BWG antenna's Ka-band link over an X-band link when the Ka-band link is optimized for maximum data return at a 30-deg elevation. Currently, the X-band links

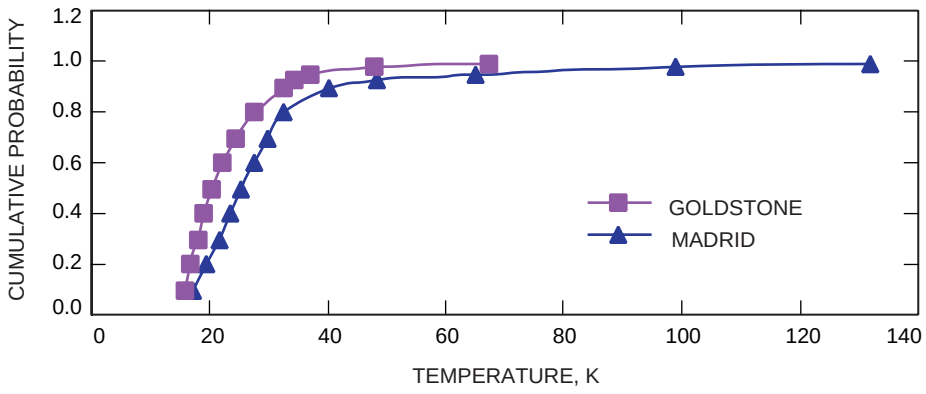

Fig. 6. Cumulative distribution of 30-deg-elevation atmospheric-noise temperature.

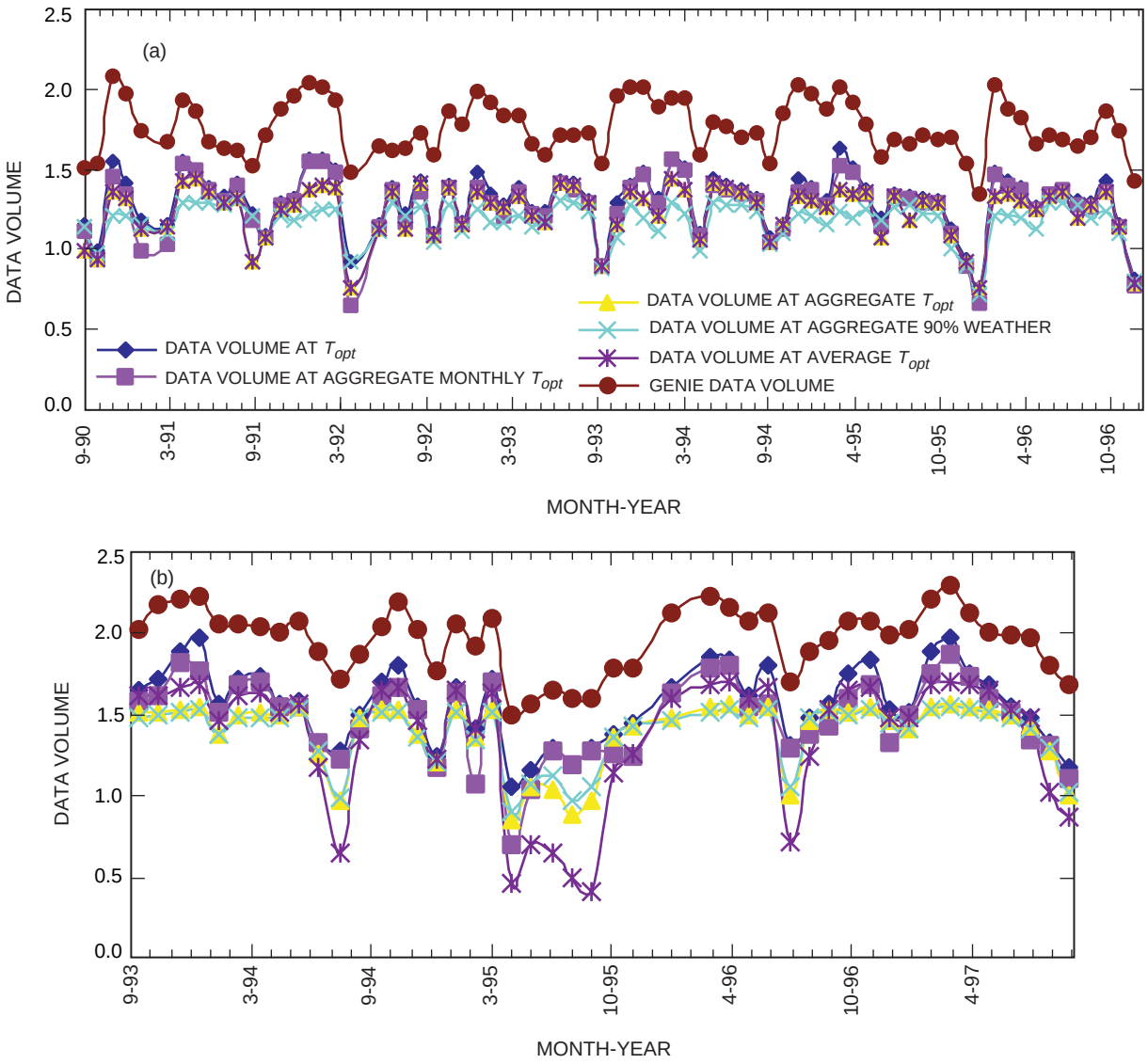

Fig. 7. Monthly genie data volume and monthly data volume for different design atmospheric-noise temperatures: (a) Madrid and (b) Goldstone.

Table 2. Average data-volume return, normalized data volume units.

Site	$\overline{V_g}$	$\overline{V_{tot}(T_{opt})}$	$\overline{V_{tot}\left(T_{opt}^{(x)}\right)}$	$\overline{V_{tot}\left(T_{opt}^{(tot)}\right)}$	$\overline{V_{tot}(\overline{T}_{opt})}$	$\overline{V_{tot}\left(T_{d}^{(90\%)}\right)}$
Madrid	1.76	1.31	1.27	1.24	1.24	1.18
Goldstone	1.97	1.57	1.48	1.39	1.37	1.39

for deep-space missions are designed for 90 percent weather. Therefore, in order to show the performance advantage of an optimized Ka-band link, in all of our comparisons we shall use X-band performance at 90 percent weather as a baseline X-band performance. Furthermore, since we do not have seasonal or monthly atmospheric noise-temperature data for X-band [4], we shall focus only on a Ka-band link that is

optimized by using $T_{opt}^{(tot)}$ in order to offer a fair comparison between the two frequencies. Two approaches are used to evaluate the Ka-band G/T advantage over X-band. Under the first approach, we calculate the data-volume advantage as a function of elevation for elevations from 9.5 to 90 deg. (Note that we have so far collected 30-deg-elevation atmospheric-noise temperature statistics; however, there is a simple conversion formula, as described in the Appendix, that allows conversion of T_{atm} from any elevation to any other elevation). In the second approach, we calculate the data-volume advantage for a typical high-elevation pass and a typical low-elevation pass and present the average data-volume advantage over the pass in dB. To calculate this advantage, we assume that transmitted power for X-band and Ka-band onboard the spacecraft is the same and that both X-band and Ka-band signals are transmitted over the same sized antennas with the exact same efficiency at their transmitting frequencies for both frequencies.

Dr. Steve Slobin of JPL has developed gain and equipment noise-temperature models as a function of elevation for the 34-m BWG antennas for both X-band and Ka-band frequencies.[3] In this article, we use these models along with the atmospheric-noise-temperature data obtained from the WVR to evaluate the return-data-volume performance advantage of Ka-band over X-band for the 34-m BWG. Figures 8(a) and 8(b) represent this advantage as a function of elevation for the 34-m BWG antennas at Madrid and Goldstone, respectively. Each figure has four curves: DPLX1, DPLX2, NDPLX1, and NDPLX2. The

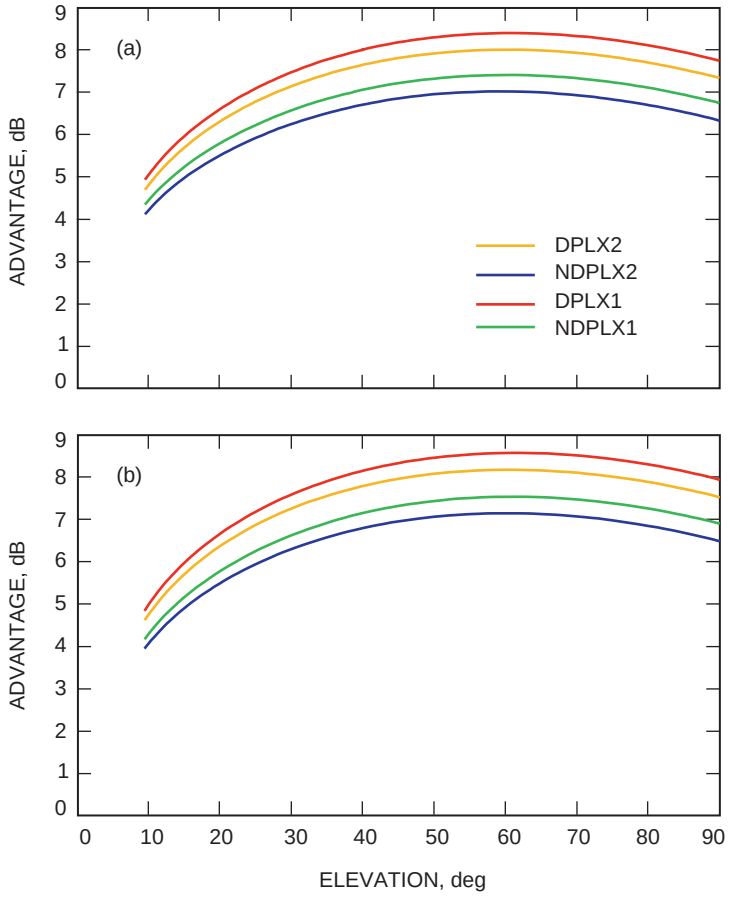

Fig. 8. The Ka-band data-volume advantage over X-band for a 34-m BWG antenna: (a) Madrid and (b) Goldstone.

[3] S. D. Slobin, "BWG Antenna Equations for Downlink Vacuum Gain and Vacuum Noise Temperature, Plus Values for Uplink Power and Gain, and Conscan Pointing Loss." JPL Interoffice Memorandum 3315-98-04 (internal document), Jet Propulsion Laboratory, Pasadena, California, January 30, 1998.

DPLX1 curve represents the performance gain when the antenna is configured to transmit an X-band uplink (i.e., the diplexer is used) and to receive only a single frequency (either X-band or Ka-band). The DPLX2 curve represents the performance gain when the antenna is configured to transmit an X-band uplink (i.e., the diplexer is used) and to receive both Ka-band and X-band frequencies. The NDPLX1 curve represents the performance advantage when the antenna is configured to receive only a single frequency and does not transmit an uplink (i.e., the diplexer is not used). The NDPLX2 curve represents the performance advantage when the antenna is configured to receive both X-band and Ka-band and does not transmit an uplink (i.e., the diplexer is not used). As seen from these figures, at low elevations, the optimized Ka-band link provides between 4 and 5 dB more data volume than does the 90 percent X-band link at both sites. At about 60 deg, the Ka-band advantage is greatest for both sites. This is due to the fact that, at a 60-deg elevation, the combination of antenna gain and atmospheric effects provides the most advantage for Ka-band over X-band. At lower elevations, the atmospheric effects cause the performance to be inferior to that at a 60-deg elevation, and, at higher elevations, antenna deformity and the reduction in gain associated with it dominate and cause a reduction in performance. Depending on the antenna configuration, this advantage at 60 deg is between 7 and 8.4 dB for both sites. Note that $T_{opt}^{(tot)}$ was used to obtain these advantage numbers. As shown in the previous section, when the aggregate monthly atmospheric-noise-temperature value, $T_{opt}^{(x)}$, is used, the Ka-band data volume increases by 0.1 dB for Madrid and 0.26 dB for Goldstone.

Figures 9 and 10 represent the performance advantage of Ka-band over X-band during high-elevation (maximum elevation ∼80 deg) and low-elevation (maximum elevation ∼30 deg) passes. The elevation trajectories of these figures were taken from actual Mars Global Surveyor Ka-band Link Experiment II (MGS/KaBLE-II) tracks at DSS 13. As we can see from these curves, the Ka-band advantage over X-band could be limited if the spacecraft is tracked at low elevations. The results for the average data-volume advantage over each pass are shown in Table 3.

As we can see from Figs. 8 through 10 and Table 3, at both sites there is a difference of approximately 1 dB in the Ka-band performance advantage between when the antenna is diplexed and when it is not. The reason is that the use of a diplexer with X-band causes an increase in the system-noise temperature. It is expected that, in the future, new diplexers will have a smaller effect on the system-noise temperature at X-band and the performance of the antenna at X-band when diplexed will be similar to its performance

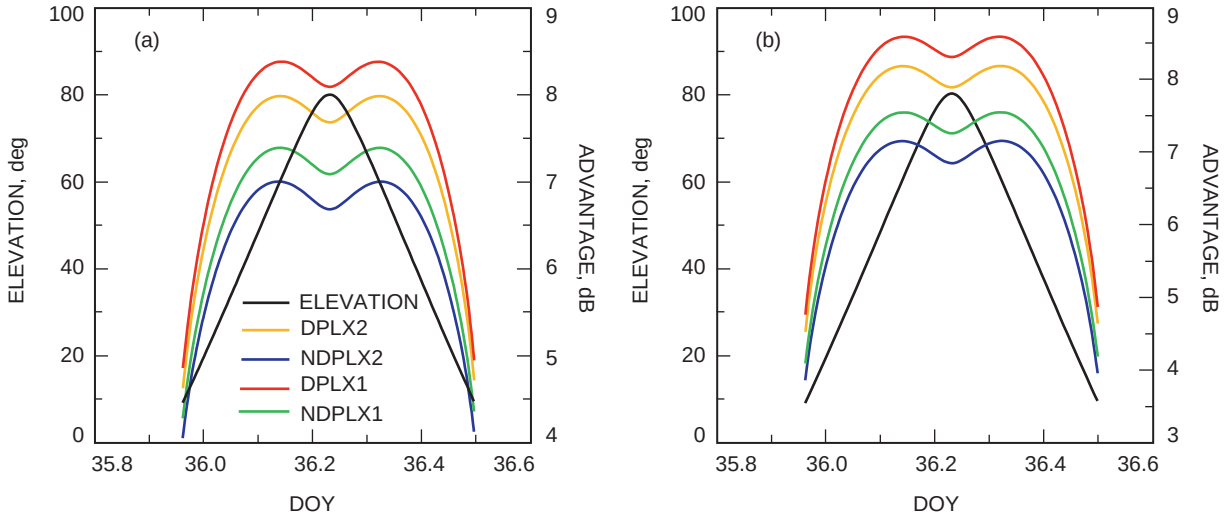

Fig. 9. The Ka-band data-volume advantage over X-band during a high-elevation pass for a 34-m BWG antenna: (a) Madrid and (b) Goldstone.

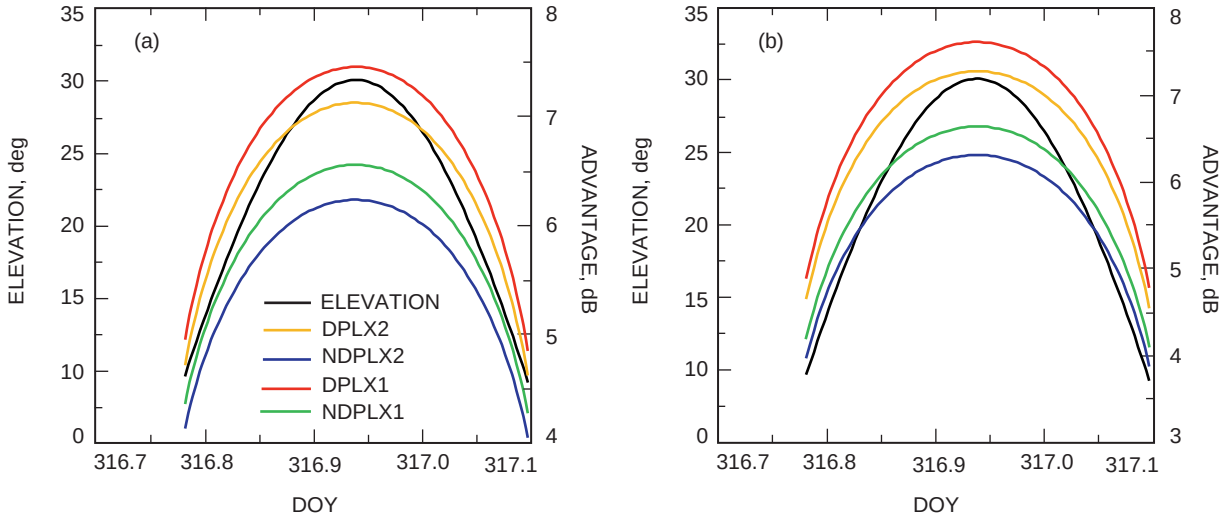

Fig. 10. The Ka-band data-volume advantage over X-band during a low-elevation pass for a 34-m BWG antenna: (a) Madrid and (b) Goldstone.

Table 3. Average Ka-band data-volume advantage over X-band for different passes.

Pass	Average DPLX1 advantage, dB	Average NDPLX1 advantage, dB	Average DPLX2 advantage, dB	Average NDPLX2 advantage, dB
Madrid, high elevation	7.8	6.8	7.4	6.5
Goldstone, high elevation	7.9	6.9	7.6	6.6
Madrid, low elevation	6.8	6.0	6.5	5.7
Goldstone, low elevation	6.9	6.0	6.6	5.7

when it is not diplexed. Furthermore, it is expected that missions will be using only a single frequency. Therefore, in the future, the performance advantage of Ka-band would most closely follow that of the NDPLX1 curves for mission design purposes. In addition, it should be noted that new X-band low-noise amplifiers (LNAs) will be installed at the 34-m BWG antennas. These new LNAs could improve the performance of X-band by as much as 1 dB. Therefore, the Ka-band advantage could be further reduced. Finally, it should be pointed out that the numbers presented here do not take into account spacecraft amplifier efficiencies and spacecraft and ground-antenna pointing. The fact that Ka-band amplifiers are not as efficient as X-band ones and that the spacecraft antenna and ground antennas are harder to point at Ka-band could reduce the Ka-band advantage presented here.

VI. Conclusions

In this article, we presented an approach to maximize the return-data volume of a link given the atmospheric-noise-temperature statistics for that link. We used this approach on the atmospheric-noise temperatures collected for a 31.4-GHz frequency at the Madrid and Goldstone Deep Space Communications Complexes and obtained the optimum atmospheric-noise temperatures that maximize the data-return volume at each complex at a 30-deg elevation. It was observed that, for both sites, the weather affects the performance of the link less than 20 percent of the time. It also was noted that Goldstone is in general drier than Madrid. It was observed that, for the complete data set at each site, the data volume is maximized at Madrid when the 84.07 percentile atmospheric-noise-temperature value of 34.00 K is

used, and it is maximized at Goldstone when the 88.78 percentile atmospheric-noise-temperature value of 31.63 K is used. Furthermore, it is noted that, if seasonal or monthly variations are taken into account, the return-data volume could be further increased. Since Goldstone experiences more seasonal variation than Madrid, taking into account the monthly and seasonal variations in the weather is more beneficial to the link at Goldstone. In addition, we used the optimum Ka-band atmospheric-noise temperature at a 30-deg elevation to calculate the return-data-volume advantage of the Ka-band link over a 90 percent weather X-band link for 34-m beam-waveguide antennas at Madrid and Goldstone for different antenna configurations at different elevations. It was observed that, depending on the configuration of the antenna, the Ka-band link provides a minimum of 4 to 5 dB more data. For both sites, at a 60-deg elevation, the Ka-band link provides between 7 and 8.4 dB more data volume than does the 90 percent X-band link, depending on the antenna configuration. Finally, we used the optimum atmospheric-noise temperature to calculate the average Ka-band return-data-volume advantage over high-elevation and low-elevation passes at both the Madrid and Goldstone sites. It was observed that, at Madrid, depending on the antenna configuration, the Ka-band link provides between 6.5 and 7.8 dB more data than does X-band for a high-elevation pass and between 5.7 and 6.8 dB more data than does X-band for a low-elevation pass. At Goldstone, the Ka-band advantage is between 6.6 and 7.9 dB for a high-elevation pass and 5.7 to 6.9 dB for a low-elevation pass.

Acknowledgments

The author would like to thank Mr. Steve Keihm of the Jet Propulsion Laboratory for providing the processed WVR data and Dr. Steve Slobin of the Jet Propulsion Laboratory for providing expert advice with regard to the 34-m BWG antenna.

References

[1] B. Sklar, *Digital Communications*, Englewood Cliffs, New Jersey: Prentice Hall, 1988.

[2] J. H. Yuen, editor, *Deep Space Telecommunications System Engineering*, New York: Plenum Press, 1983.

[3] S. D. Slobin, "Microwave Noise Temperature and Attenuation of Clouds: Statistics of These Effects at Various Sites in the United States, Alaska, and Hawaii," *Radio Science*, vol. 17, no. 6, pp. 1443–1454, November–December 1982.

[4] *DSN/Flight Project Interface Design Handbook*, vol. II, 810-5; Rev. D, Jet Propulsion Laboratory, Pasadena, California, July 15, 1992.

Appendix

Calculation of T_{atm} for Different Elevations

Let T_z be the atmospheric-noise temperature at zenith (90-deg elevation). The atmospheric-loss factor at zenith, L_z, is given by

$$L_z = \frac{275 - T_z}{275} \tag{A-1}$$

Then the atmospheric-noise temperature at elevation θ, $T_{atm}(\theta)$, is given by

$$T_{atm}(\theta) = 175 \times \left(1 - L_z^{1/\sin(\theta)}\right) \tag{A-2}$$

Using Eqs. (A-2) and (2) from the main text, we get for the atmospheric loss factor at θ, $L(\theta)$:

$$L(\theta) = L_z^{1/\sin(\theta)} \tag{A-3}$$